J Appl Electrochem (2011) 41:241–247
DOI 10.1007/s10800-010-0231-6

ORIGINAL PAPER

Electrochemical investigation of Al–Li/Li_xFePO_4 cells in oligo(ethylene glycol) dimethyl ether/$LiPF_6$

X. J. Wang · Y. N. Zhou · H. S. Lee · K. W. Nam · X. Q. Yang · O. Haas

Received: 3 January 2010 / Accepted: 15 October 2010 / Published online: 11 November 2010

Abstract 1 M $LiPF_6$ dissolved in oligo(ethylene glycol) dimethyl ether with a molecular weight, 500 g mol^{-1} (OEGDME500, 1 M $LiPF_6$), was investigated as an electrolyte in experimental Al–Li/$LiFePO_4$ cells. More than 60 cycles were achieved using this electrolyte in a Li-ion cell with an Al–Li alloy as an anode sandwiched between two Li_xFePO_4 electrodes (cathodes). Charging efficiencies of 96–100% and energy efficiencies of 86–89% were maintained during 60 cycles at low current densities. A theoretical investigation revealed that the specific energy can be increased up to 15% if conventional LiC_6 anodes are replaced by Al–Li alloy electrodes. The specific energy and the energy density were calculated as a function of the active mass per electrode surface (charge density). The results reveal that for a charge density of 4 mAh cm^{-2} about 160 mWh g^{-1} can be reached with Al–Li/$LiFePO_4$ batteries. Power limiting diffusion processes are discussed, and the power capability of Al–Li/$LiFePO_4$ cells was experimentally evaluated using conventional electrolytes.

Keywords Al–Li alloy anode · Oligo(ethylene glycol) · Al–Li/$FePO_4$ cells · Specific energy · Li diffusion in Al

X. J. Wang · Y. N. Zhou · H. S. Lee · K. W. Nam · X. Q. Yang · O. Haas (✉)
Chemistry Department, Brookhaven National Lab, Upton, NY 11973, USA
e-mail: otto.haas@bluewin.ch

Y. N. Zhou
Materials Science Department, Fudan University, Shanghai 200433, China

O. Haas
Energy and Material Research Consulting, 6648 Minusio, Switzerland

1 Introduction

Al–Li alloy electrodes have been widely investigated for Li-battery applications in various electrolyte systems [1–3]. In general, the Al–Li alloy was the active material rather than deposited lithium on top of the electrode. Al–Li electrodes were first investigated in molten salts [4] as anode materials for LiAl/FeS_2 batteries [5] or thermally activated batteries [6]. However, they were also investigated in various liquid [1, 7–10] and solid polymer electrolytes systems [11, 12] based on polyethylene oxide (PEO). The thermodynamics and the Li diffusion in Al–Li alloy were studied [13–16], and the different Al–Li stoichiometries of these alloys [13–17] as well as new preparation methods to manufacture Al–Li alloy electrodes [18] have been published. Most recently, Suresh et al. [8] published an article investigating the deposition of lithium on Al-electrodes in EC/DMC, 1 M $LiBF_4$. They claimed that the lithium deposited on aluminum is free of dendrites and thus have high potential for Li-ion battery applications.

1.1 Electrolyte system

Oligo (ethylene glycol) dimethyl ethers, which contain 10–11 ethylene glycol units (OEGDME500) are liquid solvents with high boiling points and high electrochemical stability comparable with ionic liquids but with the advantage of a lower melting point. In a previous publication, the authors investigated Al–Li alloy electrodes in this electrolyte and discovered excellent reversibility of these electrodes in OEGDME500, 1 M $LiPF_6$ [19]. At low current densities, lithium was deposited and re-dissolved at potentials more positive than those for lithium electrodes. In fact, with in situ XRD measurements, it was possible to

show that Al_1Li_1 alloy was formed during deposition of Li on aluminum.

1.2 Al–Li/Li_xFePO_4 cells

The reversibility of the Al–Li alloy electrode in OEGDME500, 1 M $LiPF_6$ and the enthusiastic report of Suresh et al. about Al–Li electrodes encouraged the authors to conduct additional investigations using this electrolyte in Al–Li/Li_xFePO_4 cells. The authors are aware of the shortcomings of Al–Li alloy anodes discussed in the review of Armand and Tarascon [20], but think that, with new electrolyte systems, improvements may still be possible.

The specific capacity of Al–Li anodes (788 mAh g^{-1}) is more than twice the specific capacity of LiC_6 anodes, and owing to the low porosities of Al–Li alloy electrodes, a lower electrolyte volume is needed in practical cells. Therefore, an increase of energy density is expected if conventional LiC_6 anodes are replaced by Al–Li alloy anodes. In this article, the authors try to quantify this aspect and discuss specific energies and power limitations as a function of the electrode capacity.

2 Experimental

2.1 Electrolyte preparation

OEGDME500 purchased from Aldrich was dissolved in dimethyl ether and passed through an activated carbon column. The ether was then evaporated, and the residue was dried at 60 °C and 0.3 mbar for 24 h. The product (OEGDME500) was stored under Ar in a dry box. 1.52 g of $LiPF_6$ was dissolved in 10 mL of OEGDME500 for about 3–4 days. The mixture was shaken from time to time until all of the salt was completely dissolved.

2.2 $LiFePO_4$ electrode preparation

$LiFePO_4$ electrodes were prepared by mixing $LiFePO_4$ with 10 wt% carbon black and 10 wt% polyvinylidene fluoride (PVDF) in *n*-methyl pyrrolidone (NMP) solution. This slurry was then spread on an aluminum foil using a blade at constant distance. The electrode was then dried in vacuum at 100 °C for several hours.

2.3 Al–Li electrode preparation

High purity Al foil (50 μm, 2.8 cm^2) was used as a starting material for the Al–Li electrode. The alloy was prepared electrochemically using the same electrochemical cell as described before [19] with the aluminum electrode sandwiched between two Li electrodes. 25 As (Coulombs) of Li^+ were slowly discharged on the aluminum electrode to form an Al–Li alloy layer on each side. Thus, the Al foil contained 2.6×10^{-4} mol Li and 1.4×10^{-3} mol Al after this treatment. A filter paper or a Cellgard membrane was used as a separator.

2.4 Li/$LiFePO_4$ and Al–Li/$LiFePO_4$ cell

The same electrochemical cells as described in [21] was used for the Li/$LiFePO_4$ experiment. For the Al–Li/$LiFePO_4$ cycle test, the 2.8 cm^2 Al–Li electrode was sandwiched between two 2.8 cm^2 $LiFePO_4$ electrodes. Thus, the total active surface area was 5.6 cm^2. The sandwich arrangement has the advantages that the current collector (Al) in the middle serves two Al–Li electrodes. The cells were typically cycled with a current of 0.2 mA, corresponding to a charge and a discharge rate of about 17.5 h at the beginning of the cycle test experiment. The capacity of the Al–Li/$LiFePO_4$ cell was 3.5 mAh. For the high power experiment, the cell capacity was 0.62 mAh.

3 Results and discussion

3.1 Cycle test

The cell with a 2.8 cm^2 Al–Li electrode sandwiched between two 2.8 cm^2 $LiFePO_4$ electrodes (described in the experimental) was submitted to a cycle test. The Al–Li electrode was prepared electrochemically by depositing 1.3×10^{-4} mol Li (3.5 mAh) on each side of a 50-μm-thick Al electrode before the cycle test, whereas the two $LiFePO_4$ electrodes each contained charge of 1.75 mAh. During cycling, the Li_xFePO_4 was completely oxidized and reduced, whereas the capacity of the Al–Li electrode was only partially used. Figure 1 shows that the Al–Li/Li_xFePO_4 cell can be cycled over many cycles. The capacity, however, decreased slowly. After 60 cycles, only about a half of the initial capacity could be used. The capacity decrease is illustrated by the charge/discharge curves of cycle 1, 2, 3; 31, 32, 33; and 61, 62, 63. Integrating the second charge–discharge curve shown in Fig. 1, we calculate a cycle charge efficiency of 99.5% and an energy efficiency of 89%, which remained almost the same over 60 cycles (insert Fig. 1) even though the capacity of the cell did declaim. The energy efficiencies after 31 and 61 cycles were still 86.3 and 85.7%, respectively. The charge efficiency varied from cycle to cycle in the range of 96–100% with the exception of the first cycle.

Because the Al–Li electrode has higher capacity than the Li_xFePO_4 electrode, the capacity loss should be caused by the Li_xFePO_4 electrode. A post mortal inspection, however, showed that the Al–Li electrode did disintegrate

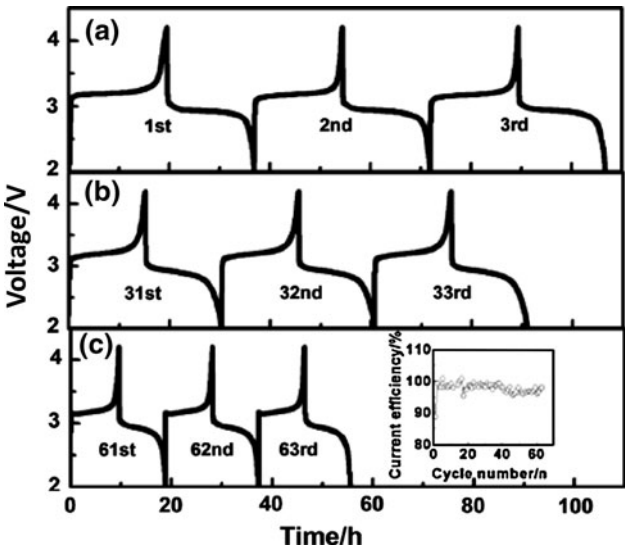

Fig. 1 Voltage response of charge/discharge cycles of an Al–Li/Li_xFePO_4 cell with sandwich arrangement using 1 M $LiPF_6$ in OEGDME500 as an electrolyte. (*a*) Cycle numbers: 1, 2, and 3. (*b*) Cycle numbers: 31, 32, and 33. (*c*) Cycle numbers: 61, 62, and 63. Current: 0.2 mA. Total electrode surface: 5.6 cm^2. *Inset*: current efficiencies of all cycles

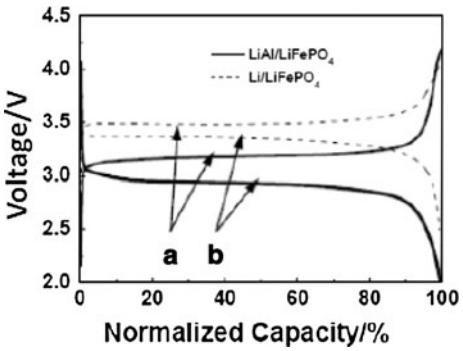

Fig. 2 Typical charge (*a*) and discharge (*b*) curves at low current densities as a function of the cell capacity and discharged capacity of an Al–Li/Li_xFePO_4 cell (electrode surface: 2.8 cm^2, two-electrode arrangement using 1 M $LiPF_6$ in OEGDME500 as an electrolyte) in comparisons with a Li/Li_xFePO_4 cell (same cell arrangement, but using 1 M $LiPF_6$ in EC/EMC as an electrolyte)

in the center having some loosely structured Al–Li alloy coagulates, which were not contacted anymore. Thus, at least toward the end of the cycle test, the capacity fade was probably due to the Al–Li electrode. The mechanical stress due to density changes during cycling may account for this structure change. To reach high cycle life, it may be advantageous to use a thin copper net to contact the disintegrating Al–Li electrode material. However, working with composite Al–Li/C electrode is probably the best solution to overcome this problem.

The voltage plateaus in the charge and discharge curves of the Al–Li/$LiFePO_4$ cell are about 350–400 mV lower than those of the Li/$LiFePO_4$ cell (Fig. 2), which confirms Al–Li alloy formation during lithium deposition in the Al–Li/$LiFePO_4$ cell. The shift in potential is due to the exergonic (negative Gibbs free energy change) reaction of Al with Li. We have almost equilibrium potentials at these low current densities and may therefore use the potential difference (0.375 V) to make a rough estimate of the free energy of the Al–Li alloy formation. With $\Delta G = -zF\Delta E = -36$ kJ mol^{-1}, we obtain a value, which corresponds well with published data: -8.9 kcal mol^{-1} [9, 22], and 0.38 eV [20]. Measurements in molten salts like LiCl–KCl give somewhat lower value of -28.6 kJ mol^{-1}, which is due to higher temperatures (427 °C). In these electrolytes, Li_3Al_2 alloy with $\Delta G = -58$ kJ mol^{-1} is also produced [23]. We have no evidence for the formation of alloys with different stoichiometries [24] other than Li_1Al_1. The in situ XRD investigation [19] and the ex situ investigations of Suresh et al. [8] done by the authors showed only XRD pattern of Al_1Li_1 alloy, suggesting that other alloys were either not produced or produced only in minor amounts.

Figure 2 shows a clear potential difference for the charge/discharge curves of an Al–Li/Li_xFePO_4 cell and a Li/Li_xFePO_4 cell. In the Al–Li/Li_xFePO_4 cell, these two curves are separated by about 260 mV—just about twice as much as for the Li/Li_xFePO_4 cell, which was cycled in a conventional electrolyte (1 M $LiPF_6$ in EC/EMC). From the voltage separation of the charge/discharge curve, we deduce an internal resistance of 330 Ω for the Li/Li_xFePO_4 cell, and about 650 Ω for the Al–Li/Li_xFePO_4 cell.

3.2 Lithium location in the aluminum electrode

At the used current densities in our cycle test, the entire deposited lithium is incorporated into the bulk of the Al electrode. The diffusion coefficients for Li in aluminum and Al–Li alloys are probably within 10^{-8}–10^{-10} cm^2 s^{-1} (see discussion in Part I [19]). Assuming a diffusion coefficient of 10^{-9} cm^2 s^{-1}, the diffusion length for Li in the electrode during 17.5 h (time of the first charging period) corresponds to 115 μm. The deposited lithium should, therefore, be distributed all over the electrode thickness. (N.B. both sides of the 50-μm aluminum electrode are plated simultaneously).

3.3 Engineering aspects

The potential loss due to alloy formation, which was about 375 mV compared to a Li/$LiFePO_4$ cell (see Fig. 1) or about 200 mV compared to a LiC_6/$LiFePO_4$ cell, is more than compensated by the higher specific capacity of the Al–Li alloy (788 mAh g^{-1}), which is more than twice the theoretical specific charge of LiC_6 (372 mAh g^{-1}). As mentioned before, an energy density increase is also

expected since the Al–Li electrodes have almost no porosities if the alloying process is started with a compact aluminum electrode. The Al–Li electrode serves as current collector and active electrode material, which helps also to economize both weight and space. The Al–Li electrode, however, needs a surplus of alloyed lithium to ensure that some of the lithium will be able to diffuse back to the surface in time when the cell is discharged.

To quantify the advantage of Al–Li alloy electrodes compared with commonly used LiC_6 electrodes, we calculated the specific energy and the energy densities of Al–Li/Li_xFePO_4 and LiC_6/Li_xFePO_4 cells as a function of nominal capacities, where the nominal capacity would be the practical useable capacity of the cell. All the parameters used for this investigation are listed in Table 1. In Table 2, the numerical results of the specific energies and energy densities are listed as a function of the nominal capacity, and Table 3 presents the calculated weights and dimensions of the cell components and of all the cells. Figure 3 visualizes the data listed in Tables 2 and 3. In the upper part of Fig. 3, the development of the specific energy and the energy density is shown as a function of the nominal capacity. In the lower part, the development of the cell dimensions is visualized for the indicated nominal capacities.

It should be mentioned that the thickness of the Al–Li alloy layers listed in Table 3 correspond to the theoretical thickness assuming that this layer consists of a pure Al_1Li_1 alloy. In practice, the lithium will diffuse deeper into the aluminum electrode.

Table 1 Parameters used to calculate the specific energies and energy densities listed in Table 2 and visualized in Fig. 3

	Material properties
Spec. weight, electrolyte	1.1 g cm^{-3}
Spec. weight, Cu	8.92 g cm^{-3}
Spec. weight, Al	2.7 g cm^{-3}
Spec. weight, Al–Li layer	1.72 g cm^{-3}
Spec. weight, Li_xFePO_4	3.577 g cm^{-3}
Spec. weight, LiC_6	2.25 g cm^{-3}
Spec. weight, membrane	0.85 g cm^{-3}
Capacity/g, Al–Li alloy	2838 As g^{-1}
Capacity/g, $LiFePO_4$	486 As g^{-1}
Capacity/g, LiC_6	1080 As g^{-1}
Porosity, Al–Li layer	0.1 cm^3 cm^{-3}
Porosity, Li_xFePO_4	0.5 cm^3 cm^{-3}
Porosity, LiC_6	0.5 cm^3 cm^{-3}
Porosity, membrane	0.4 cm^3 cm^{-3}
Thickness, Cu	0.001 cm
Thickness, Al	0.0025 cm
Thickness, membrane	0.0025 cm
Voltage, LiC_6/Li_xFePO_4	3.6 V
Voltage, Al–Li/Li_xFePO_4	3.4 V
Housing	20%

For the calculations of this study, we used 10% excess of $LiFePO_4$ and LiC_6 electrodes and 30% excess of lithium in the Al–Li electrode. The electrolyte volume was assumed to be equal to the total pore volume of the electrodes and the membrane. The electrode thickness has been calculated assuming 50% porosity of the LiC_6 and $LiFePO_4$, electrode, and 10% porosity of the Al–Li electrode layer. The porosity of the membrane was assumed to be 40%, which is typical for Cellgard membranes. An additional weight and volume of 20% was also used for the battery housing.

Using the data given in Table 1, the specific weight of the cells is in the range of 2.24–2.53 g cm^{-3} for the cells with LiC_6 electrodes, and 2.29–2.39 g cm^{-3} for the cells with the Al–Li electrodes.

The data in Table 2 show that, independent of the nominal capacity, the specific energies of the Al–Li/Li_xFePO_4 cells are always higher than those for the LiC_6/Li_xFePO_4 cells. This is also the case for the energy densities; however, owing to the thinner copper foil (10 μm) compared to the Al foil (25 μm) for the nominal capacity 1 mAh cm^{-2}, the LiC_6/$LiFePO_4$ cell has a slightly higher energy density. At a nominal capacity of 4 mAh cm^{-2}, the specific energy is close to 160 mWh g^{-1} for Al–Li/Li_xFePO_4 cells, which is about 15% higher than that for LiC_6/Li_xFePO_4 cells. The specific energy could still be increased using higher nominal capacities, however, this would lead to electrodes with rather thick Li_xFePO_4 layers (>182 μm) and slow diffusion. With a nominal capacity of 4 mAh cm^{-2} it should still be possible to reach attractive power densities.

For a discharge rate of 1 h with a layer of 182-μm-thick Li_xFePO_4, if we assume a particle size of $d = <0.1$ μm, a diffusion rate in the particles $\geq 10^{-14}$ cm^2 s^{-1} and a conductivity in the Li_xFePO_4 film of about 4×10^{-4} S cm^{-1} should be possible [25]. For a 1-h discharge rate of a cell with nominal capacity of 4 mAh cm^{-2}, the supply of Li^+ ions should reach 0.00015 mol cm^{-2} h^{-1}. Concerning the diffusion of Li^+ in the electrolyte, we have to be aware of the fact that with a porosity of 50% the Li_xFePO_4 concentration in the Li_xFePO_4 layer is about 11 M. As the Li concentration in the electrolyte is only 1 M, the electrolyte salt has to be replaced 22 times during a 1 h discharge rate. Using the following formula, we may estimate whether the replacement of Li ions is fast enough to reach the necessary current density:

$$i = nF \frac{dc}{dx} \frac{D_{Li+}}{1-t_+} \frac{1}{\tau}$$

where $n = 1$, $F = 96500$ As, $D_{Li+} = 10^{-6}$ cm^2 s^{-1}, transference number $t_+ = 0.4$, tortuosity factor $\tau = 2.8$,

Table 2 Numerical results of specific energies and energy densities of LiC_6/Li_xFePO_4 and Al–Li/Li_xFePO_4 cells for nominal capacities: 1, 2, 3, and 4 mAh cm^{-2}

Nominal capacity (mAh cm^{-2})	Specific energy		Energy density	
	LiC_6/Li_xFePO_4 (mAh g^{-1})	$AlLi/Li_xFePO_4$ (mAh g^{-1})	LiC_6/Li_xFePO_4 (mAh cm^{-3})	$AlLi/Li_xFePO_4$ (mAh cm^{-3})
1	82.3	86.9	208.5	207.3
2	112.7	124.4	266.3	290.3
3	128.5	145.3	293.4	334.9
4	138.2	158.7	309.2	362.9

Table 3 Necessary weight (g cm^{-2}) and thicknesses of the active electrode materials used for Al–Li/Li_xFePO_4 and LiC_6/Li_xFePO_4 cells with nominal capacities: 1, 2, 3, and 4 mAh cm^{-2}

Nominal capacity	1 mAh cm^{-2}		2 mAh cm^{-2}		3 mAh cm^{-2}		4 mAh cm^{-2}	
Active material/cell	g	cm	g	cm	g	cm	g	cm
Al–Li	0.00165	0.0011	0.00330	0.0021	0.00495	0.0032	0.00660	0.0043
Li_xFePO_4	0.00815	0.0046	0.01630	0.0091	0.02444	0.0137	0.03259	0.0182
LiC_6	0.00367	0.0033	0.00733	0.0065	0.01100	0.0098	0.01467	0.0130
LiC_6/Li_xFePO_4 cell	0.03501	0.0138	0.05112	0.0216	0.06723	0.0295	0.08335	0.0373
Al–Li/Li_xFePO_4 cell	0.03131	0.0131	0.04373	0.0187	0.05615	0.0244	0.06857	0.0300

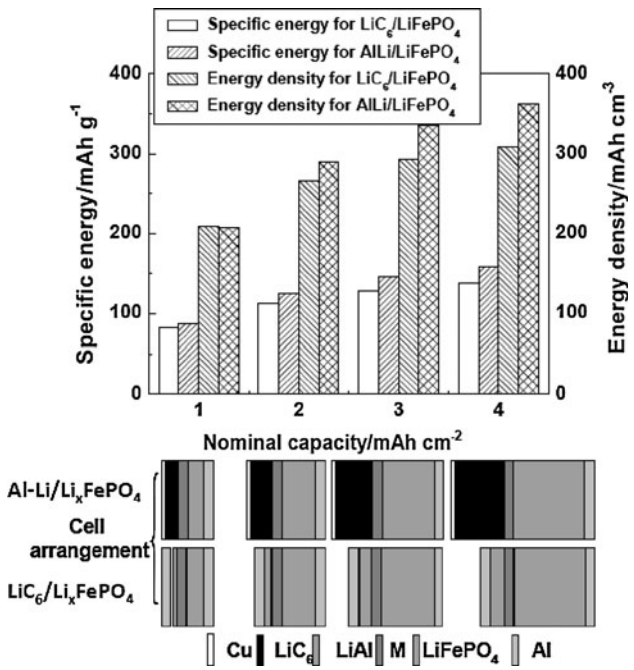

Fig. 3 Comparison of the specific energy with the energy density as a function of the nominal capacity of Al–Li/Li_xFePO_4 and LiC_6/Li_xFePO_4 cells. *Lower part*: cell dimensions for Al–Li/Li_xFePO_4 and Li C_6/Li_xFePO_4 cells for the same nominal capacities used in the upper part of the figure. The calculations include 10% overcapacity for the LiC_6 and Li_xFePO_4 electrodes and 30% for the Al–Li electrode. It also includes 20% weight and volume for housing. The electrolyte volume was assumed to be the same as the total pore volume of the cell, where the porosity was assumed to be 50% for LiC_6, 50% for Li_xFePO_4, 10% for the Al–Li, and 40% for the membrane (M)

$dc/dx = 0.05$ mol cm^{-4}, $dx = 0.0207$ cm (182-μm Li_xFePO_4 electrode thickness + 25 μm membrane thickness), and $dc = 0.001$ mol cm^{-3}. Assuming $[Li^+] = 1$ M at the Al–Li or LiC_6 electrode surface and ~0 M at its current collector underneath of the porous Li_xFePO_4 electrode mass, we estimate a flow rate of Li^+ ion of 2.9×10^{-8} mol cm^{-2} and a current density of 2.8 mA cm^{-2}, which means that the discharge would need about 1.4 h. However, at the beginning of the discharge the concentration gradient will be much higher as the Li^+ ions would have already been used off within a thin layer at the surface of the Li_xFePO_4 electrode. However, toward the end of discharge, 2.8 mA cm^{-2} will be the highest possible current density.

The diffusion of Li in the Al–Li electrode is not included in the above. Depending on the diffusion coefficient, it may be slower. The diffusion length after 1 h would be 85 μm with a diffusion coefficient of 10^{-8} cm^2 s^{-1}, which would allow a sufficient supply of Li^+ ions if the charge transfer at the surface is fast enough. With a diffusion coefficient of 10^{-10} cm^2 s^{-1}, the diffusion length in 1 h would only be 8.5 μm. With this diffusion rate the Li^+ ion supply could just be sufficient if the Al–Li electrode would contain an excessive amount of Li. Even with $D = 10^{-8}$ cm^2 s^{-1}, it will be advantageous to have a certain excess of Li in the Al–Li electrode to prevent slowing down of the diffusion from the bulk to the surface at the end of discharge. As mentioned in part I [19], different data have been published concerning the Li diffusion coefficient in Al–Li electrodes. The diffusion coefficient depends also

strongly on the concentration of lithium in the Al–Li alloy [26]. Published diffusion rates range from 10^{-10} cm^2 s^{-1} [19] to 8×10^{-8} cm^2 s^{-1} [10, 15, 27, 28].

Little is known about the heterogeneous rate constant to quantify the charge transfer at the Al–Li electrode surface and the Li_xFePO_4 grain surfaces. Oxide layers or decomposition products of the electrolyte can have a huge influence on the heterogeneous reaction rate. Such effects will show up as an over potential leading to a lower cell potential noted already at the beginning of the discharge process. With a particle size of about 0.1 μm, the total particle surface of the 182-μm-thick Li_xFePO_4 layer would be about 5500 cm^2 for a Li_xFePO_4 electrode of 1 cm^2. This large active surface area helps us to compensate for a presumably low heterogeneous rate constant.

At low capacities (e.g., 1 mAh cm^{-2}), the expected discharge rates are much more attractive also regarding the Li_xFePO_4 electrode. Using the same assumptions as used above it should be possible to discharge a half of the cell in less than 10 min. However, the theoretical specific energy drops to 87 mWh g^{-1}, and even less at high discharge rates. Figure 4 shows some experimental data collected with a low capacity Al–Li/Li_xFePO_4 cell using conventional carbonate electrolytes (unfortunately with the use of OEGDME500, 1 M $LiPF_6$ as an electrolyte, such a high discharge rate cannot be achieved). Figure 4 shows that with 0.2 mA, the cell is discharged within 3 h, whereas with 2 mA, the cell is discharged within about 15 min, where the capacity is only decreased by about 15%. From the difference in voltage plateaus between the charge/discharge curves, we calculate an internal resistance of about 90 Ω during the 3-h discharge rate and, about 400 Ω for the 15-min discharge rate. The experiments shown in Fig. 4 clearly demonstrate that fast discharge rates are possible for Al–Li/Li_xFePO_4 cells with low capacities.

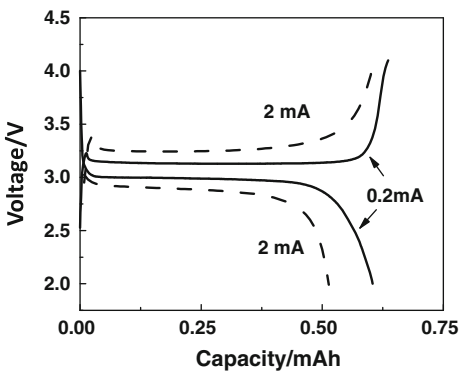

Fig. 4 Charge/discharge curves of a low capacity Al–Li/Li_xFePO_4 cell. Cell capacity: 0.62 mAh; Electrode surface: 2.8 cm^2; Electrolyte: 1 M $LiPF_6$ in EC/EMC; Current: 2 mA and 0.2 mA corresponding to discharge rates of 15 min and 3 h, respectively

Even though the above discussion about current densities and obtainable power densities may have rather a big uncertainty it still gives an idea about the power ability of Al–Li/Li_xFePO_4 cells, and the experimental data shown in Fig. 4 confirm that the estimates are not completely out of range. More precise estimates could be obtained with numerical simulations; however, as the diffusion constants and the heterogeneous rate constants are not well known, numerical calculations would not lead to more accurate results.

4 Conclusions

The experimental investigation of an Al–Li/Li_xFePO_4 cell using OEGDME500, 1 M $LiPF_6$ as an electrolyte reveals high energy and charge efficiencies for this cell at low current densities. The cell potential at low current densities is about 375 mV lower than that of a comparable Li-$FePO_4$ cell, which is because of the exergonic Al–Li alloy formation. The cell did survive more than 60 cycles, but with decreasing capacities. Half of the original capacity was retained after 60 cycles. A comparison of a Al–Li/Li_xFePO_4 cell with a LiC_6/Li_xFePO_4 cell reveals a possible increase in the specific energy of about 15% if LiC_6 electrodes are replaced by Al–Li electrodes and specific energies close to 160 mAh g^{-1} are not unrealistic but the discharge of such cells with a capacity of about 4 mAh cm^{-2} will be rather slow when MPEG500, $LiPF_6$ is used as an electrolyte. Discharge rates considerably less than 1 h can be reached with Al–Li/Li_xFePO_4 cells using conventional electrolytes (EC/EMC, 1 M $LiPF_6$) with capacities of the order of 1 mAh cm^{-2}. The specific energy of such a cell, however, is much lower about 80 mAh g^{-1}. At such low capacities, the inactive parts of the cell attenuate the specific energy of the cell.

Acknowledgments This study was supported by the Assistant Secretary for Energy Efficiency and Renewable Energy, Office of Vehicle Technologies, under the program of "Hybrid and Electric Systems," of the U. S. Department of Energy under Contract Number DEAC02-98CH10886. We would also like to thank the China Scholarship Council for the financial support in favor of Y. N. Zhou.

References

1. Geronov Y, Zlatilova P, Moshitev RV (1984) J Power Sources 12:145
2. Besenhard J (1977) J Electroanal Chem 78:1490
3. Ding F, Liu Y, Hua X (2006) Electrochem Solid-State Lett 9:A72
4. Melendres CA (1977) J Electrochem Soc 124:650
5. Gay EC, Vissers DR, Martino FJ, Anderson KE (1976) J Electrochem Soc 123:1591
6. Guidotti RA, Masset PJ (2008) J Power Sources 183:388
7. Besenhard J (1978) J Electroanal Chem 94:77

8. Suresh P, Shukla AK, Shivashankar SA, Munichandraiah N (2004) J Power Sources 132:166
9. Epelboin I, Froment M, Garreau M, Thevenin J, Warin D (1980) J Electrochem Soc 127:2100
10. Jow TR, Liang CC (1983) J Electrochem Soc 129:1429
11. Maskell WC, Owen JR (1985) J Electrochem Soc 132:1602
12. Bang HJ, Kim S, Prakash J (2001) J Power Sources 92:45
13. Rao BML, Francis RW, Christopher MA (1977) J Electrochem Soc 124:1490
14. Garreau M, Thevenin J, Warin D, Campion P (1980) In: Yeager EB et al (eds) Proceedings of the workshop on lithium non-aqueous battery electrochemistry, vol 80-7. The Electrochemistry Society, Pennington, USA, June 4–6, p 158
15. Baranski AS, Fawcett WR (1982) J Electrochem Soc 129:901
16. Kumagai N, Kikuchi Y, Tanno K, Lantelme F, Chemla M (1992) J Appl Electrochem 22:728
17. Hamon H, Topart P, Brousse T, Buvat P, Jousse F, Schleich DM (2001) J Power Sources 97–98:185
18. Moshtev RV, Zlatilova P, Puresheva B, Manev V, Kozawa A (1994) J Power Sources 51:409
19. Zhou YN, Wang XJ, Lee HS, Nam KW, Yang XQ, Haas O (2010) J Appl Electrochem. doi:10.1007/s10800-010-0233-4
20. Tarascon JM, Armand M (2001) Nature 414:359
21. Yoon WS, Chung KY, McBreen J, Fischer DA, Yang XQ (2007) J Power Sources 174:1015
22. Nicholson MM (1974) J Electrochem Soc 121:736
23. Selman JR, DeNuccio DK, Sy CJ, Steunenberg RK (1977) J Electrochem Soc 124:1160
24. McAlister AJ (1982) Bull Alloy Phase Diagr 3:177
25. Wang D, Li H, Shi S, Huang X, Chen L (2005) Elctrochim Acta 50:2955
26. Kishio K, Britain JO (1979) J Phys Chem Solids 40:933
27. Willhite JR, Karnezos N, Christea P, Brittain JO (1976) J Phys Chem Solids 37:1073
28. Lantelme F, Iwadate Y, Shi Y, Chemla M (1985) J Electrochem Soc 187:229